

This article was downloaded by: [University of Haifa Library]

On: 08 August 2012, At: 14:05

Publisher: Taylor & Francis

Informa Ltd Registered in England and Wales Registered Number: 1072954 Registered office: Mortimer House, 37-41 Mortimer Street, London W1T 3JH, UK



Molecular Crystals and Liquid Crystals

Publication details, including instructions for authors and subscription information:

<http://www.tandfonline.com/loi/gmcl20>

Elastic Anisotropy and Anchoring Effects on the Textures of Nematic Films with Random Planar Surface Alignment

Cesare Chiccoli^a, Paolo Pasini^a & Claudio Zannoni^b

^a INFN, Sezione di Bologna, Bologna, Italy

^b Dipartimento di Chimica Fisica ed Inorganica and INSTM-CRIMSON, Bologna, Italy

Version of record first published: 22 Feb 2010

To cite this article: Cesare Chiccoli, Paolo Pasini & Claudio Zannoni (2010): Elastic Anisotropy and Anchoring Effects on the Textures of Nematic Films with Random Planar Surface Alignment, Molecular Crystals and Liquid Crystals, 516:1, 1-11

To link to this article: <http://dx.doi.org/10.1080/15421400903396944>

PLEASE SCROLL DOWN FOR ARTICLE

Full terms and conditions of use: <http://www.tandfonline.com/page/terms-and-conditions>

This article may be used for research, teaching, and private study purposes. Any substantial or systematic reproduction, redistribution, reselling, loan, sub-licensing, systematic supply, or distribution in any form to anyone is expressly forbidden.

The publisher does not give any warranty express or implied or make any representation that the contents will be complete or accurate or up to date. The accuracy of any instructions, formulae, and drug doses should be independently verified with primary sources. The publisher shall not be liable for any loss, actions, claims, proceedings, demand, or costs or damages whatsoever or howsoever caused arising directly or indirectly in connection with or arising out of the use of this material.

Elastic Anisotropy and Anchoring Effects on the Textures of Nematic Films with Random Planar Surface Alignment

CESARE CHICCOLI,¹ PAOLO PASINI,¹
AND CLAUDIO ZANNONI²

¹INFN, Sezione di Bologna, Bologna, Italy

²Dipartimento di Chimica Fisica ed Inorganica and INSTM-CRIMSON,
Bologna, Italy

We present a Monte Carlo study of topological defects in nematic films with random planar boundary conditions. The polarized microscopy images and their evolution are analysed in uniaxial systems for different anchoring strengths and film thicknesses.

Keywords Biaxial nematics; computer simulation; Monte Carlo; topological defects

Introduction

Monte Carlo simulations of lattice spin models have revealed useful in studying Liquid Crystals ordering and phase transitions in the bulk and in confined systems [1]. For instance, we have shown that this technique is useful in investigating sub-micron droplets with fixed (radial and planar) surface anchoring mimicking polymer dispersed liquid crystals (PDLC) [2,3], twisted nematic displays [4] and thin nematic films [5,6]. The large number of particles which can be currently simulated on a lattice ($10^5 - 10^6$) allows us also to simulate the optical textures, as can be obtained by a polarized microscopy experiment, with a sufficient number of pixels. The prototype model for this kind of investigations is the Lebwohl-Lasher (LL) one [7,8] which was the first lattice system put forward to successfully simulate the orientational properties of a nematic. This model has obtained a great success because, despite its simplicity, it captures the essential orientational properties of a nematic and of its clearing transition [8]. One of the limitations of the model is that it yields the three elastic constants as equal, as the potential contains only one, scalar, interaction energy term [9]. We have shown in various papers that also in this one-constant approximation some of the characteristics of nematics, like the creation of topological defects in confined systems, can be reproduced using Monte Carlo computer simulations [5,6,10].

Address correspondence to Paolo Pasini, INFN, Sezione di Bologna, Via Irnerio 46, Bologna 40126, Italy. E-mail: pasini@bo.infn.it

While for low molar mass liquid crystals the differences between the K_i elastic constants are normally small [11], the need for accounting in a simple way the effect of different elastic constants is particularly important for various systems where the elastic constants are likely to differ considerably. In particular, large differences in elastic constants can be expected in polymer liquid crystals [12,13] or in liquid crystals originated from long virus like TMV [14], nanotubes [15] or other nanocrystal suspensions [16].

Establishing a direct relation between molecular structure and elastic constants or even just predicting relative changes in elastic constants following changes in molecular structure would be of great importance, but has proved a considerably difficult task even if some approximate treatments exist.

For instance, deGennes [17] observed long time ago that splay distortion should be unlikely to occur, and correspondingly K_1 should be very large for systems of long rods, because of the crowding of rods at one end caused by splay. This was experimentally observed by Sun Zheng Min and Kleman [18] who found for a main chain polyester $K_1 = 3 \times 10^{-12} \text{ N} \approx 10 K_3$. For another polyester Volino *et al.* [19] found $K_1 \approx 2-3 K_3$. Considering approximate analytical formulas for the free elastic energy of the different types of defects Kleman [12] noticed long time ago that two brushes (topological charge $s=1/2$) defects should be favored. We discussed this in [10] when considering the possibility of using the observation of two brushes defects as a test of nematic biaxiality as suggested by Chandrashekar [20].

Assuming phase uniaxiality, measuring geometrical features such as disclination radii of the $s=1/2$ defects has been suggested as a means to determine at least some elastic constants in polymer liquid crystals from Transmission Electron Microscopy (TEM) images. In particular Hudson and Thomas [21] found in this way the elastic anisotropy $\varepsilon = (K_1 - K_3)/(K_1 + K_3)$ to vary from negative (-0.15) to positive ($+0.20$) in two very similar hydroquinone based polymer. TQT10H and TQT10M differing only by a replacement of a hydrogen with a methyl. Incidentally this shows that it is extremely difficult to make prediction on elastic constants based on similarity of molecular structures, differently from simple expectation such as that of deJeu *et al.* that $K_1:K_2:K_3 = 1:1:(l/w)^2$ for a molecule of length l and width w [22]. Given the importance of relating elastic constant to texture a number of numerical treatments based on minimization of the continuum free energy have put forward, particularly by Windle and coworkers for polymer liquid crystals [23] and by Killian, Hess *et al.* [24].

Going back to microscopic simulations, the introduction of biaxial contributions [25,26] or other more complex spatially anisotropic interactions [27,28] in the pair potential potentially lifts the degeneracy of elastic constants of the simple LL model. However, as elastic constants are not directly predictable from the microscopic model they would have to be calculated as observable properties, a task of considerable difficulty in itself [27,28]. If the aim is, like here, a study of the effect of elastic constants of the topological defects in nematic films this would imply modifying the pair potential in a more or less arbitrary way, and calculating on one hand defects and on the other elastic constants and other related observables such as order parameters. Thus since elastic constants and defects are in this fully microscopic approach both observables (i.e., and results of the simulation) establishing a relation between them is a rather indirect process. A much more direct approach has been provided by Gruhn and Hess [29] and Romano and Luckhurst [30,31] by introducing

a pseudo pair potential that directly depends on classic splay, twist and bend elastic constants K_1 , K_2 , K_3 .

Here we wish to show that a simple application of the Gruhn-Hess-Romano-Luckhurst pseudopotential [29–31] coupled with Monte Carlo simulations can be a very effective way to treat the onset of textures and their evolution in a variety of situations. We concentrate in particular on thin uniaxial films with random planar (Schlieren) conditions and study a number of cases with various elastic constant anisotropies.

The Model Systems

The Gruhn-Hess-Romano-Luckhurst model [29–31] consists of a system of interacting centers (“spins”) placed at the sites of a certain regular lattice, here taken as cubic. The Hamiltonian is written as follows:

$$U_N = (1/2) \sum_{\substack{i,j \in F \\ i \neq j}} \Phi_{i,j} + J \sum_{\substack{j \in S \\ j \in S}} \Phi_{ij} \quad (1)$$

where F , S are the set of particles in the bulk and at the surfaces, respectively, and the parameter J models the strength of the coupling with the surfaces. The particles interact through the second rank attractive pair potential:

$$\begin{aligned} \Phi_{ij} = \epsilon_{i,j} \{ & \lambda [P_2(\mathbf{u}_j \cdot \mathbf{s}) + P_2(\mathbf{u}_k \cdot \mathbf{s})] + \mu [(\mathbf{u}_j \cdot \mathbf{s})(\mathbf{u}_k \cdot \mathbf{s})(\mathbf{u}_j \cdot \mathbf{u}_k) - 1/9] + \nu P_2(\mathbf{u}_j \cdot \mathbf{u}_k) \\ & + \rho [P_2(\mathbf{u}_j \cdot \mathbf{s}) + P_2(\mathbf{u}_k \cdot \mathbf{s})] P_2(\mathbf{u}_j \cdot \mathbf{u}_k) \} \end{aligned} \quad (2)$$

Where $\epsilon_{ij} = \epsilon$ for nearest neighbors and zero otherwise, determines the interactions strength and

$$\begin{aligned} \lambda &= (1/3)\Lambda(2K_1 - 3K_2 + K_3); \\ \mu &= 3\Lambda(K_2 - K_1); \\ \nu &= (1/3)\Lambda(K_1 - 3K_2 - K_3); \\ \rho &= (1/3)\Lambda(K_1 - K_3) \end{aligned}$$

with K_1 , K_2 , K_3 the splay, bend and twist elastic constants. Λ is a factor which, for dimensional consistency, has the dimension of a length. The vectors \mathbf{s} and \mathbf{r} are defined as follows: $\mathbf{s} = \mathbf{r}/|\mathbf{r}|$, $\mathbf{r} = \mathbf{x}_j - \mathbf{x}_k$, with \mathbf{x}_j , \mathbf{x}_k dimensionless coordinates of the j -th and k -th lattice points. \mathbf{u}_j , \mathbf{u}_k are unit vectors along the axis of the two particles (“spins”) and P_2 is a second rank Legendre polynomial. Notice that the pseudo-pair potential Eq. (2), although it has formally the same mathematical structure of the LL one, is temperature dependent through the elastic constants K_i . Moreover, as far as interpretation goes, in the original microscopic models the spins represent a cluster of neighboring molecules whose short range order is assumed to be maintained through the temperature range examined [1]. Here \mathbf{u}_i , \mathbf{u}_j , \mathbf{r} represent similarly the local director at two neighbouring sites i, j separated by vector \mathbf{r} . In the one constant approximation as a special case, i.e., $\lambda = \mu = \rho = 0$, reduces to the simple Lebwohl-Lasher (LL) potential [8,9]. While in simulating bulk systems [32] periodic boundary conditions are employed, in the case of confinement the boundaries

are implemented by considering additional layers of particles, kept fixed during the simulation, with suitable orientations chosen to mimic the desired surface alignment [33].

Here we present an investigation of uniaxial nematic films with “Schlieren” random planar simulated and study the effect of varying elastic constants, anchoring and film thickness. To start with, we consider, however, the one-constant approximation case [5,10]. In this and in the rest of numerous cases treated in the paper, the starting configurations of the lattice are chosen to be completely aligned along the z direction and the evolution of the system is followed according to the classic Metropolis Monte Carlo procedure [34].

Polarizing microscope textures were simulated by means of a Müller matrix approach [35], assuming the molecular domains represented by the spins to act as retarders on the light propagating through the sample observed between crossed polarizers [36].

Simulations and Results

The following parameters were employed for computing the optical textures: film thickness $d = 5.3 \mu\text{m}$, ordinary and extraordinary refractive indices $n_o = 1.5$ and $n_e = 1.66$, and light wavelength $\lambda_o = 545 \text{ nm}$.

As mentioned before we have investigated uniaxial films with different anchoring at the surfaces and now we report results for the various cases studied.

The first case we present is a $100 \times 100 \times (10 + 2)$ system in a Schlieren geometry, where the orientations of the “surface spins” are random and planar at the top and bottom surfaces. We analyze the effect of the anchoring coupling strength on the creation and evolution of defects (Fig. 1 in the one-constant approximation (LL model)).

We see from Figure 1 that the system evolves from the initial dark state to various somewhat different textures. It can be noticed that, for this thickness, a coupling with the surfaces of the same strength of the nematic-nematic interaction (i.e., $J = 1$) is not sufficient to maintain the network of defects which is created after a few thousands of MC cycles. In other words, for this anchoring and thickness, the surface seems to dominate over the system. We have checked that this is the case also for higher values of interactions with the surfaces, i.e., $J = 1.5$ and $J = 2.0$ (the results are not shown for reasons of space). Decreasing the coupling with the surface the MC simulations show instead that a typical coarsening network presents mainly defects with four dark brushes and thus strength $k = \pm 1$ (the director rotates by 2π around the defect center), Figure 1 [10]. The defects tend then to disappear by pair annihilation $+1-1=0$ after longer simulation cycles [10]. The defects $k = \pm 1$ are not singular, as the local director \mathbf{n} reorients along the vertical axis [10]. In contrast to the well known “escape into third dimension” in a cylindrical sample [37] surface anchoring at the bounding plates hinders reorientation by forming a pair of point defects-boojums capping the line at the plates [10]. Reducing again the coupling with the surfaces the number of defects created in the sample decreases until reaching a complete absence of defects when the anchoring strength is very low (Fig. 1, bottom row), $J = 0.1$. In that case the ordering effect of the potential dominates the disordering effect of the boundary conditions and, at the low temperature deep in the nematic phase at which the simulations have been performed, the whole systems tend to be aligned along a preferred direction, the z one of the starting configuration.

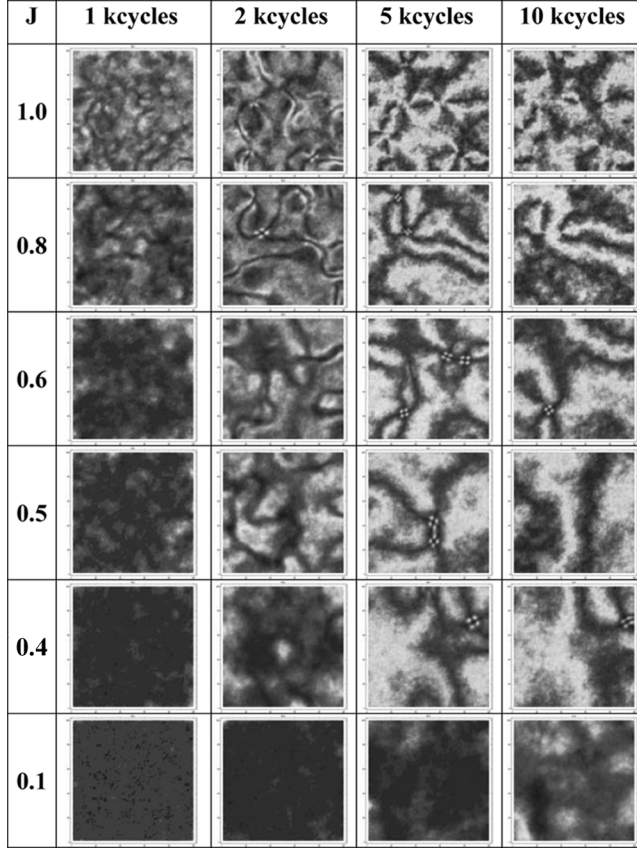


Figure 1. Simulated polarized microscopy images of a LL ($K_1 = K_2 = K_3$) uniaxial nematic film in a Schlieren geometry as obtained from Monte Carlo configurations. The images are taken after 1000, 2000, 5000, and 10000 MC cycles with the sample between crossed polarizers. The system size is $100 \times 100 \times 12$, the reduced temperature is $T^* = 0.4$ and the anchoring coupling with the surfaces are $J = 1, 0.8, 0.6, 0.5, 0.4, 0.1$.

These considerations can be quantitatively confirmed by looking at the values of the order parameter $\langle P_2 \rangle$ calculated for the whole system: they are lower when the number of defects is larger. For example the values of $\langle P_2 \rangle$ correspondent to the cases presented in Figure 1, last column from the top, are the following $J = 1.0$, $\langle P_2 \rangle = 0.42$; $J = 0.8$, $\langle P_2 \rangle = 0.57$; $J = 0.6$, $\langle P_2 \rangle = 0.31$; $J = 0.5$, $\langle P_2 \rangle = 0.28$; $J = 0.4$, $\langle P_2 \rangle = 0.54$ and $J = 0.1$, $\langle P_2 \rangle = 0.66$.

Fairly similar results can be obtained by increasing the thickness of the film which corresponds to an interaction with the surfaces increased by about the same multiplicative factor. This is evident from the results shown in Figure 2 where the defects observed for $J = 0.5$ appear for a $100 \times 100 \times 22$ system when the coupling is $J = 1$.

Focusing on a coupling $J = 0.5$ we have then investigated a system with the same geometry where different combinations of the elastic constants values have been taken into account.

The results, reported in Figures 3–8, show how the different elastic constants contribute to the appearance of defects. It is clear that a moderate increase of the

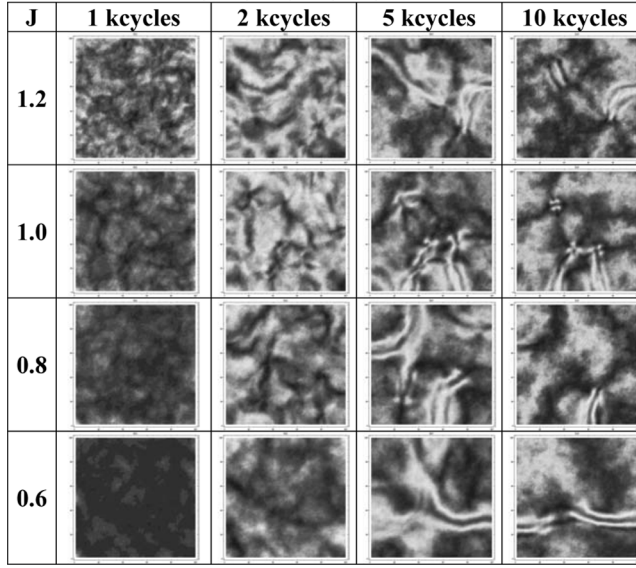


Figure 2. As in Figure 1 for a system size $100 \times 100 \times 22$.

strength of one of the splay or bend (K_1 and K_3) constant over the other two (v. Fig. 3) favours the appearance of four brushes defects, while increasing only the twist elasticity no defect is created.

However, when the strength of K_1 is further increased and becomes much higher than the other ones (see Fig. 4, first row) the splay distortion does not induce the formation of defects. On the contrary the singularities are still created with a very strong bend constant (see Fig. 4, last row).

The importance of the K_1 and K_3 with respect to K_2 in the formation of defects is also evident by looking at the results shown in Figure 5–8 where all the cases with different combination of the three elastic constants taken into account are presented. It is clear that a high value of K_2 does not allow a creation of defects as it is for a very strong splay constant in comparison with the twist and bend ones.

Examining the pseudo-potential in Eq. (2) it is apparent that it depends linearly on K_i , so that a scaling factor ξ , for which $K_i = \xi K'_i$ can be absorbed in ε . This in turn means that the temperature as appearing in the Monte Carlo Boltzmann average becomes $T^* = kT/\varepsilon = kT/(\varepsilon\xi) = T'\xi$. In other words, when all the elastic constants are scaled by the same amount, the textures correspond to a similar system with a different ordering. For this reason even though the textures are to some extent invariant to a scaling factor such as ξ we give explicit values for all three K_i in the figures.

Apart from the ideal case values studied we have also performed simulations for experimental elastic constant data taken from literature [38,39] for the 5CB, MBBA, and TMV.

The results are shown in Figure 9 and we can notice that the texture can be compared with the test cases here presented. It is evident that the defects appear when the bend and splay constants are approximately of the same strength and stronger than the twist one (5CB and MBBA). The case of the Tobacco Mosaic Virus is less clear because two brushes defects seem to be created.

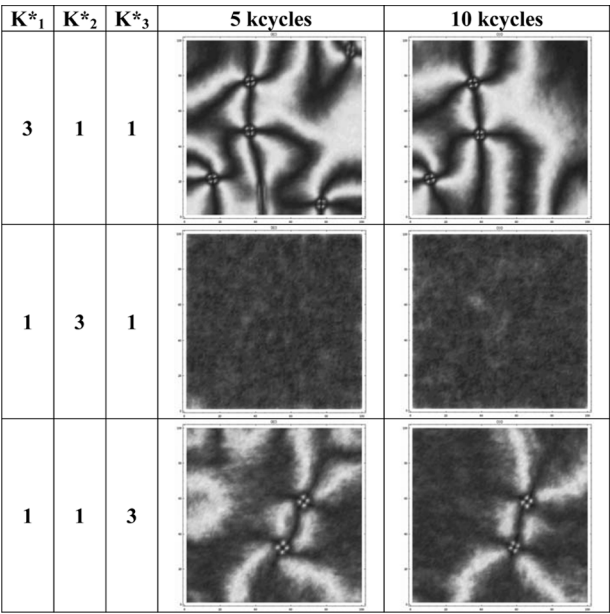


Figure 3. Simulated optical patterns for a nematic film in a Schlieren geometry as obtained from a Monte Carlo simulation of a Gruhn-Hess potential for different values of the three elastic constants. The images are taken after 5000 and 10000 MC cycles with the sample between crossed polarizers. The system size is $100 \times 100 \times 12$, the reduced temperature is $T^* = 0.4$ and the anchoring coupling with the surfaces is $J = 0.5$. The values of the elastic constants $K_i = K_i^* \times 10^{-12} \text{ N}$ taken into account are reported in the first three columns.

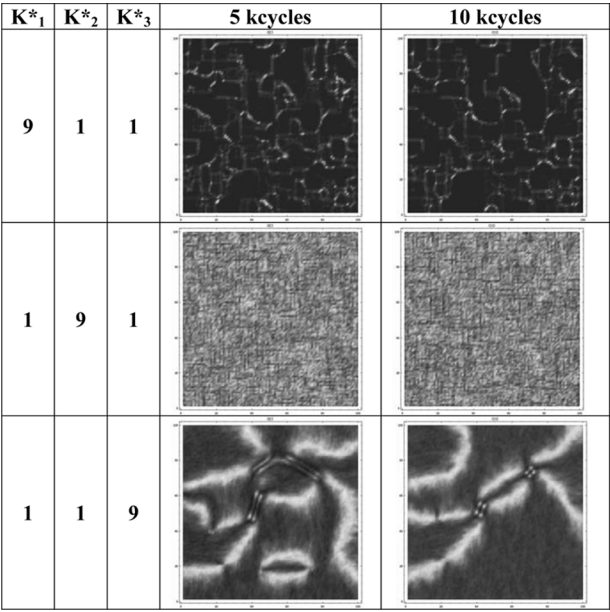


Figure 4. As in Figure 3 for higher values of the elastic constants $K_i = K_i^* \times 10^{-12} \text{ N}$.

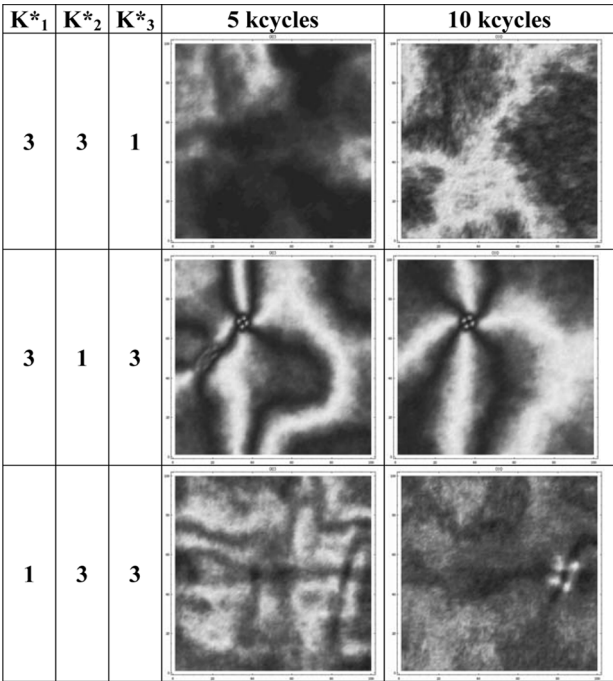


Figure 5. As in Figure 3 for higher values of the elastic constants $K_i = K_i^* \times 10^{-12}$ N.

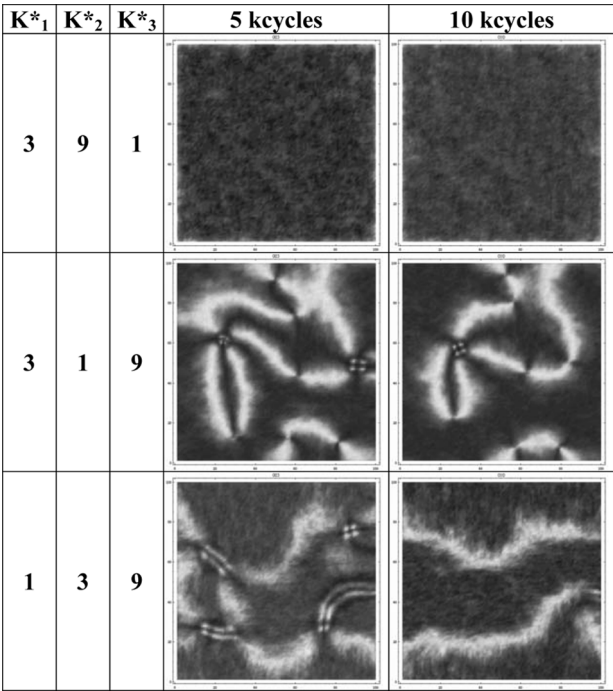


Figure 6. As in Figure 3 for higher values of the elastic constants $K_i = K_i^* \times 10^{-12}$ N.

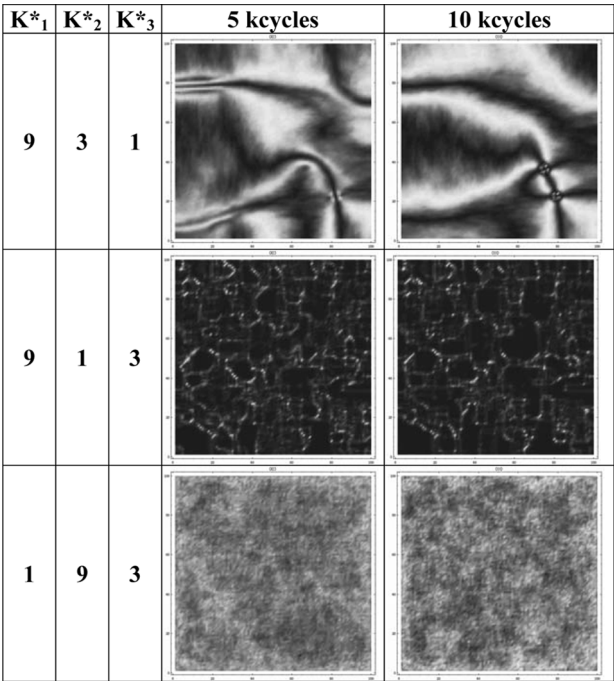


Figure 7. As in Figure 3 for higher values of the elastic constants $K_i = K^*_i \times 10^{-12} \text{ N}$.

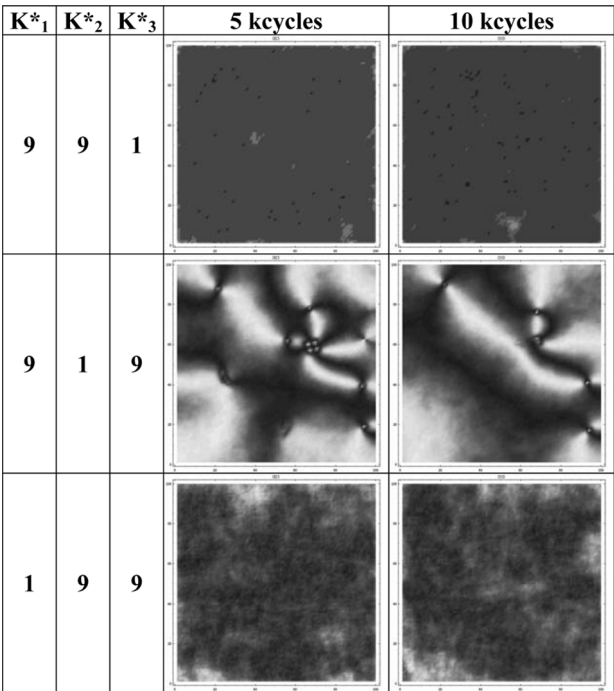


Figure 8. As in Figure 3 for higher values of the elastic constants $K_i = K^*_i \times 10^{-12} \text{ N}$.

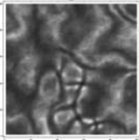
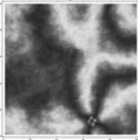
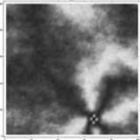
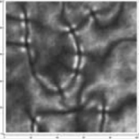
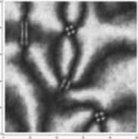
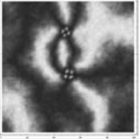
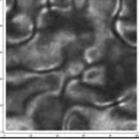
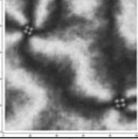
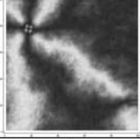
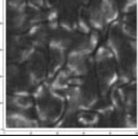
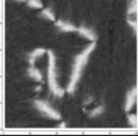
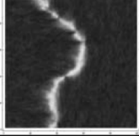
K^*_1	K^*_2	K^*_3	2 kcycles	5 kcycles	10 kcycles
7.0	4.4	9.7			
6.4	3.6	8.2			
1.0	0.6	1.6			
1.0	0.22	8.8			

Figure 9. Simulated optical patterns for a nematic film in a Schlieren geometry as obtained from a Monte Carlo simulation of a Gruhn-Hess potential for different values of the three elastic constants as taken from experimental results. The values correspond to 5CB and MBBA from Ref. [38] (first and second row, respectively), MBBA and TMV from Ref. [39] (third and fourth row, respectively). The images are taken after 2000, 5000, and 10000 MC cycles with the sample between crossed polarizers. The system size is $100 \times 100 \times 12$, the reduced temperature is $T^* = 0.4$ and the anchoring coupling with the surfaces is $J = 0.5$. The values of the Elastic constants $K_i = K^*_i \times 10^{-12}$ N taken into account are reported in the first three columns.

Conclusions

We have performed a detailed simulation study of a nematic film with random planar boundary condition by using a simple Gruhn-Hess-Romano-Luckhurst pseudo-potential which take into account the elastic anisotropy of the system. We have considered different combinations of the elastic constants to verify their relative importance on the formation of various optical patterns.

We have shown that the bend and splay anisotropies are responsible of the creation of defects which are not allowed when the twist distortion dominates. We notice that some of the considerations reported here could be obtained by comparing the explicit expressions for free energy of the various types of defects in the bulk [12,23]. However the simple technique reported here allows a simple consideration of the effect of boundary conditions and thickness.

References

- [1] Pasini, P. & Zannoni, C. (Eds.) (2000). *Advances in the Computer simulations of Liquid Crystals*, Kluwer: Dordrecht.
- [2] Chiccoli, C., Pasini, P., Semeria, F., & Zannoni, C. (1990). *Phys. Lett. A*, 150, 311.

- [3] Berggren, E., Zannoni, C., Chiccoli, C., Pasini, P., & Semeria, F. (1994). *Phys. Rev. E*, 49, 614.
- [4] Chiccoli, C., Guzzetti, S., Pasini, P., & Zannoni, C. (2001). *Mol. Cryst. Liq. Cryst.*, 360, 119.
- [5] Chiccoli, C., Lavrentovich, O. D., Pasini, P., & Zannoni, C. (1997). *Phys. Rev. Lett.*, 79, 4401.
- [6] Chiccoli, C., Feruli, I., Pasini, P., & Zannoni, C. (2001). In: *Defects in Liquid Crystals: Computer Simulations, Theory and Experiments*, Lavrentovich, O. D., Pasini, P., Zannoni, C., & Žumer, S. (Eds.), Kluwer: Dordrecht, Ch. 4.
- [7] Lebwohl, P. A. & Lasher, G. (1972). *Phys. Rev. A*, 6, 426.
- [8] Fabbri, U. & Zannoni, C. (1986). *Mol. Phys.*, 58, 763.
- [9] Zannoni, C. (1986). *J. Chem. Phys.*, 84, 424.
- [10] Chiccoli, C., Feruli, I., Lavrentovich, O. D., Pasini, P., Shiyonovskii, S., & Zannoni, C. (2002). *Phys. Rev. E*, 66, 030701.
- [11] Stannarius, R. (1998). In: *Handbook of Liquid Crystals. Low Molecular Weight Liquid Crystals I*, Demus, D. & Goodby, J. et al. (Eds.), Wiley-VCH: Weinheim, Vol. 2A, 60.
- [12] Kleman, M. (1991). In: *Liquid Crystallinity in Polymers. Principles and Fundamental Properties*, Ciferri, A. (Ed.), VCH: New York, 365.
- [13] Song, W. H., Tu, H. J., Goldbeck-Wood, G., & Windle, A. H. (2003). *Liq. Cryst.*, 30, 775.
- [14] Hurd, A. J., Fraden, S., Lonberg, F., & Meyer, R. B. (1985). *J. de Physique*, 46, 905.
- [15] Song, W. H., Kinloch, I. A., & Windle, A. H. (2003). *Science*, 302, 1363.
- [16] Li, L. S., Walda, J., Manna, L., & Alivisatos, A. P. (2002). *Nano Lett.*, 2, 557.
- [17] de Gennes, P. G. (1977). *Mol. Cryst. Liq. Cryst. Lett.*, 34, 177.
- [18] Sun Zheng, Min & Kleman, M. (1984). *Molec. Cryst. Liq. Cryst.*, 3, 321.
- [19] Martins, A. F., Esnault, P., & Volino, F. (1986). *Phys. Rev. Lett.*, 57, 1745; Esnault, P. et al. (1990). *Liq. Cryst.*, 7, 607.
- [20] Chandrasekhar, S. et al. (1998). *Current Science*, 75, 1042.
- [21] Hudson, S. D. & Thomas, E. L. (1989). *Phys. Rev. Lett.*, 62, 1993.
- [22] De Jeu, W. H. (1981). *Mol. Cryst. Liq. Cryst.*, 63, 83.
- [23] Hobdell, J. & Windle, A. H. (1995). *Liquid Crystals*, 19, 401; (1997). 23, 157.
- [24] Sonnet, A., Kilian, A., & Hess, S. (1995). *Phys. Rev. E*, 52, 718; Kilian, A. & Hess, S. (1989). *Z. Naturforsch.*, 44a, 693.
- [25] Luckhurst, G. R. & Romano, S. (1980). *Mol. Phys.*, 40, 129.
- [26] Biscarini, F., Chiccoli, C., Pasini, P., Semeria, F., & Zannoni, C. (1995). *Phys. Rev. Lett.*, 75, 1803.
- [27] Allen, M. P., Warren, M. A., Wilson, M. R., Sauron, A., & Smith, W. (1996). *J. Chem. Phys.*, 105, 2850.
- [28] Stelzer, J., Bates, M. A., Longa, L., & Luckhurst, G. R. (1997). *J. Chem. Phys.*, 107, 7483.
- [29] Gruhn, T. & Hess, S. (1996). *Z. Naturforsch.*, A51, 1.
- [30] Romano, S. (1998). *Int. J. Mod. Phys. B*, 12, 2305.
- [31] Luckhurst, G. R. & Romano, S. (1999). *Liq. Cryst.*, 26, 871.
- [32] Ref. [1]. Ch. 5.
- [33] Ref. [1]. Ch. 6.
- [34] Metropolis, N., Rosenbluth, A. W., Rosenbluth, M. N., Teller, A. H., & Teller, E. (1953). *J. Chem. Phys.*, 21, 1087.
- [35] Killian, A. (1993). *Liq. Cryst.*, 14, 1189.
- [36] Ondris-Crawford, R., Boyko, E. P., Wagner, B. G., Erdmann, J. H., Žumer, S., & Doane, J. W. (1991). *J. Appl. Phys.*, 69, 6380.
- [37] Cladis, P. E. & Kleman, M. (1972). *J. Phys.*, Paris, 33, 591.
- [38] Dunmur, D. A. (2001). In: *Physical Properties of Liquid Crystals: Nematics*, Dunmur, D. A. & Fukuda, A. et al. (Eds.), INSPEC, IEE: London, Vol. 25, 216.
- [39] Hurd, A. J., Fraden, S., Lonberg, F., & Meyer, R. B. (1985). *J. de Physique*, 46, 905.